

Use of Density Functional Calculations To Predict the Regioselectivity of Drugs and Molecules Metabolized by Aldehyde Oxidase

Rhonda A. Torres,^{*,†,‡} Kenneth R. Korzekwa,^{*,§} Daniel R. McMasters,[†] Christine M. Fandozzi,[§] and Jeffrey P. Jones^{*,‡}

Department of Molecular Systems, Merck Research Laboratories, Rahway, New Jersey 07065, Department of Drug Metabolism, Merck Research Laboratories, West Point, Pennsylvania 19468, and Department of Chemistry, Washington State University, Pullman, Washington 99164

Received March 28, 2007

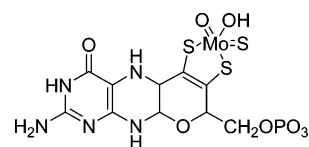
Aldehyde oxidase is a molybdenum hydroxylase that catalyzes the oxidation of aldehydes and nitrogen-containing heterocycles. The enzyme plays a dual role in the metabolism of physiologically important endogenous compounds and the biotransformation of xenobiotics. Using density functional theory methods, geometry optimization of tetrahedral intermediates of drugs and druglike compounds was examined to predict the likely metabolites of aldehyde oxidase. The calculations suggest that the lowest energy tetrahedral intermediate resulting from the initial substrate corresponds to the observed metabolite $\geq 90\%$ of the time. Additional calculations were performed on a series of heterocyclic compounds where the products resulting from metabolism by xanthine oxidase and aldehyde oxidase differ in many instances. Again, the lowest energy tetrahedral intermediate corresponded to the observed product of aldehyde oxidase metabolism $\geq 90\%$ for the compounds examined, while the observed products of xanthine oxidase were not well predicted.

Introduction

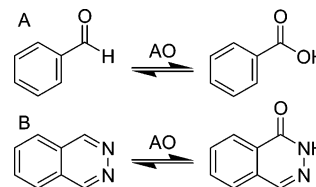
Oxidative biotransformations of xenobiotics are mediated primarily by cytochrome P450 isoforms and non-P450 enzymes including flavin monooxygenase, monoamine oxidase, alcohol dehydrogenase, and the molybdenum hydroxylases.¹ Currently, aldehyde oxidase (AO^a) is not a major drug metabolizing enzyme; however, as stated by Obach, "As efforts in drug design strive to reduce or remove cytochrome P450 metabolic liability, new drugs will be cleared by other mechanisms, such as aldehyde oxidase."² At present, the efforts to reduce cytochrome P450 metabolic liability have increased the number of azaheterocyclic structures tested for their potential as new drug entities. Replacing a carbon in an aromatic ring with a nitrogen decreases the electron density in the aromatic ring carbons, thereby decreasing P450-mediated aromatic oxidation. These electron-deficient carbons then become susceptible to nucleophilic attack by AO. The recent attention given to this enzyme^{2–4} attests to AO's growing significance. Furthermore, the potential for toxicity in humans increases whenever an animal model is unable to predict metabolic pathways. For example, dogs have no liver AO, mice have three different AO enzymes, while humans have a single AO gene.⁵ Given the species differences in metabolism, computational models may point to potentially misleading animal modeling of metabolic routes and toxicity.

In addition to AO, there are a number of enzymes containing a molybdenum pyranopterin cofactor (Scheme 1) that share a basic biochemistry important in human homeostasis, including xanthine oxidase (XO) and sulfite oxidase. While many studies (described below) have elucidated the inorganic chemistry of these molybdenum-containing oxidases, our knowledge of

Scheme 1. Structure of the Molybdenum Pyranopterin Cofactor (MoCo)



Scheme 2. Oxidase Products of Aldehyde Oxidase^a



^a Reaction A is benzaldehyde oxygenation, and reaction B is phthalazine oxygenation.

reactivity and mechanism changes with different small druglike molecules is almost nonexistent. While the physiological function of XO is well-known, that of AO is not.⁵ One possible function is the oxidation of retinal to retinoic acid, but this has not been confirmed.⁶ Genetic evidence has also linked AO to the familial recessive form of amyotrophic lateral sclerosis (ALS).⁷ This leads to possible toxic interactions in humans due to disrupted homeostasis.

The general mechanism of aldehyde oxidase is largely inferred from studies on xanthine oxidase. These enzymes can oxygenate compounds including aldehydes and azaheterocycles to carboxylic acids or, for example, phthalazinones as shown in Scheme 2. Both AO and XO have the ability to oxidize a number of different structures, from small bicyclic compounds to complicated structures with multiple ring systems. Most druglike molecules studied thus far are substrates for AO and show limited affinity for human XO.^{4,8–10}

Xanthine oxidase and aldehyde oxidase contain similar binding sites, have similar molecular properties, and exhibit broad substrate specificity with some overlap between them. The oxidation involves cleavage of a C–H bond and, in

* To whom correspondence should be addressed. For R.A.T.: phone, 509-335-1516; e-mail, rhonda.torres@yahoo.com. For K.R.K.: e-mail, korzekwa@allchemie.net. For J.P.J.: phone, 509-335-5983; e-mail, jpp@wsu.edu.

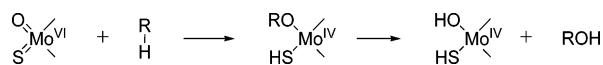
[†] Department of Molecular Systems, Merck Research Laboratories.

[‡] Washington State University.

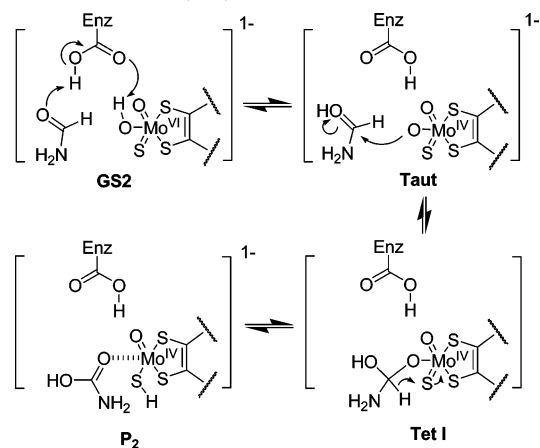
[§] Department of Drug Metabolism, Merck Research Laboratories.

^a Abbreviations: AO, aldehyde oxidase; XO, xanthine oxidase; MoCo, molybdenum pyranopterin cofactor; ALS, amyotrophic lateral sclerosis; DFT, density functional theory.

Scheme 3



Scheme 4. Stepwise Nucleophilic Attack of MoCo on Formamide Followed by Hydride Transfer



aromatic heterocyclic compounds, generally occurs adjacent to a nitrogen atom; the resulting product does not remain in the enol form, shown in Scheme 3, but rapidly converts to the keto form.

A number of studies have been performed on the mechanism of electron transfer in XO, and by inference AO, by the Hille,¹¹ Enemark,¹² and Massey¹³ groups. Briefly, the source of oxygen in the product is water; nucleophilic attack and hydride transfer leave the substrate coordinated to the MoCo, and the enzyme is reduced. A buildup of reduced enzyme, with or without the substrate bound to the MoCo by C–O–Mo bonds, is observed (Scheme 4). Finally, electrons are transferred from the MoCo to the iron–sulfur clusters and then to the flavin as has been observed by EPR. The final reduction product for AO is superoxide or hydrogen peroxide. The production of reactive oxygen species is believed to be the connection between AO and ALS.⁷ The overall reaction generates reducing equivalents in contrast to the cytochrome P450 isoforms, where reducing equivalents are consumed and molecular oxygen is the source of oxygen incorporation into the resulting product.

Oxidation via AO or XO results in metabolites that differ from those that occur during metabolism with the cytochromes P450 monooxygenases. Metabolites generated via the action of AO are being observed more often in drug metabolism as increasingly electron-deficient molecules are synthesized to decrease metabolism by cytochrome P450 isoforms. For the cytochromes P450, a number of publications exist that predict the site(s) of metabolism in a compound, assuming the compound is a substrate.^{14–16} AO typically oxidizes at carbon atoms adjacent to N atoms; however, the electron-deficient substrates of AO usually have more than one N atom and, therefore, multiple plausible oxidation sites. There are currently no methods available in the literature to predict regioselectivity of a molecule by AO, and reliable computational predictions of likely products and/or potential liabilities as early as possible in drug development are desirable. If simple computational methods can be developed for predicting the regioselectivity of AO metabolism, they can be used to redesign molecules to slow metabolism. This is particularly important when a compound is rapidly excreted or oxidized to a toxic metabolite. Herein, we describe a simple, qualitative method using density

functional theory (DFT) to predict the product of AO metabolism by examining the energetics of likely tetrahedral intermediates resulting from nucleophilic attack on carbon.

Results

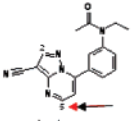
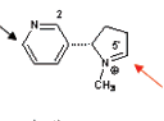
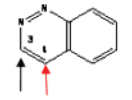
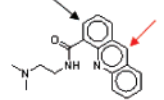
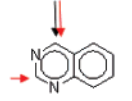
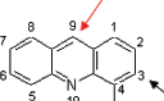
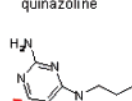
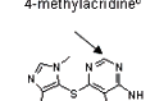
It has been suggested that a potential predictor of the site of AO metabolism for a compound is the most positively charged carbon adjacent to nitrogen in an aromatic ring. In addition, steric effects have also been suggested to influence the observed products.¹⁷ Geometry optimizations of the substrate and product of AO metabolism were performed in an effort to discern if the carbon with the highest partial charge in the heteroaromatic ring system determined the site of metabolism. As can be seen in Table 1, the charges do not appear to be predictive. Obviously, a different approach is required to enhance our predictive capacity.

Given that the first step in the proposed mechanism for AO is nucleophilic attack, the tetrahedral intermediate resulting from the oxygenation reaction by AO at each carbon was examined. The use of the tetrahedral intermediate as a means of predicting the resulting oxidation product reflects the proposed reaction mechanism for this enzyme and the observation of a tetrahedral intermediate in the crystal structure of the closely related XO complexed with the slow-metabolizing substrate FYX-051.¹⁸ While evidence exists for a concerted nucleophilic attack, and hydride transfer, the position of metabolism may still be dictated by the energy of the tetrahedral intermediate. As the reaction is identical for each compound and is believed to proceed via a common mechanism, the relative energies of the tetrahedral intermediates are proportional to the activation enthalpies of the reactions as described by the Hammond postulate.¹⁹

The energies of the likely tetrahedral intermediates of eight drug molecules that have been reported as AO substrates in the literature are presented in Table 1. In nearly every instance, the tetrahedral intermediate with the lowest ΔG_{rel} corresponded to the observed metabolic product of AO; the exception here was deoxypenciclovir. For deoxypenciclovir the observed metabolite is addition at the 6-position, while computation predicts oxidation at the 8-position. One possible explanation for the incorrect prediction is the formation of an intramolecular hydrogen bond in the geometry-optimized structure of the **8oh** deoxypenciclovir intermediate. As shown in Figure 1a, the –OH of the tetrahedral intermediate on C8 forms a hydrogen bond with an alcohol on the side chain connected to the N9, with an O–H distance of 1.9 Å and O–H···O angle of 168.8°. This is a stabilizing interaction, but it is unlikely to occur in the enzyme active site since it would likely result in unfavorable van der Waals contact with the cofactor and enzyme. This hydrogen bonding interaction does not occur in the **6oh** intermediate (Figure 1b).

A number of proprietary compounds with pre-existing AO metabolism data were examined computationally via this method to determine if the lowest energy tetrahedral intermediate resulting from nucleophilic attack on carbon corresponded to the observed product. The results of this comparison are given in Table 2. In this table, compounds with the same number are structurally related, while those with different numbers are structurally diverse. For each druglike molecule in this table, the tetrahedral intermediate with the lowest energy corresponded to the observed product. This trend was also predicted for truncated model compounds, compounds in which the substituents extending off the heteroaromatic ring system were truncated in an effort to reduce computational effort while maintaining the inherent functionality of the substituent.²⁰

Table 1. Relative Energy Comparisons^a between Likely Tetrahedral Intermediates^b of Known Substrates Metabolized by Aldehyde Oxidase

Substrate	Site of Oxidation	Substrate	Site of Oxidation
 zaleplon	2oh $\Delta G_{rel} = +16.12$ kcal/mol 5oh $\Delta G_{rel} = 0$ kcal/mol	 nicotine	2oh $\Delta G_{rel} = +9.89$ kcal/mol 6oh $\Delta G_{rel} = +7.34$ kcal/mol 5'oh $\Delta G_{rel} = 0$ kcal/mol
 cinnoline	3oh $\Delta G_{rel} = +14.49$ kcal/mol 4oh_n1h $\Delta G_{rel} = 0$ kcal/mol 4oh_c3h $\Delta G_{rel} = +12.56$ kcal/mol	 DACA	3oh $\Delta G_{rel} = +14.49$ kcal/mol 9oh $\Delta G_{rel} = 0$ kcal/mol
 quinazoline	2oh_n1h $\Delta G_{rel} = +1.69$ kcal/mol 2oh_n3h $\Delta G_{rel} = +14.76$ kcal/mol 4oh $\Delta G_{rel} = 0$ kcal/mol	 4-methylacridine ^c	3oh $\Delta G_{rel} = +18.99$ kcal/mol 9oh $\Delta G_{rel} = 0$ kcal/mol
 deoxy penciclovir	6oh $\Delta G_{rel} = +0.73$ kcal/mol 8oh $\Delta G_{rel} = 0$ kcal/mol	 azathioprine	2oh_n1h $\Delta G_{rel} = +12.64$ kcal/mol 2oh_n3h $\Delta G_{rel} = +15.97$ kcal/mol 8oh $\Delta G_{rel} = 0$ kcal/mol

^a In kcal/mol. ^b Red \uparrow = site of metabolism. Black \uparrow = most positive carbon in ring. ^c Truncated model of compound in series where the metabolite is predicted.

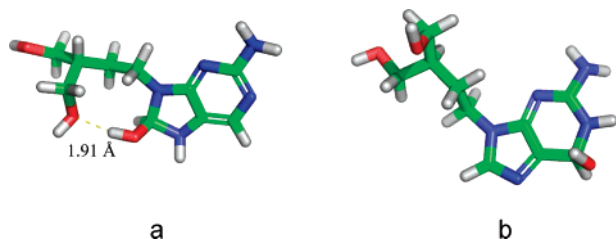


Figure 1. (a) Structure of deoxy penciclovir tetrahedral intermediate **8oh** showing hydrogen bond between $-OH$ on C8 and substituent on N9. (b) Structure of deoxy penciclovir tetrahedral intermediate **6oh**.

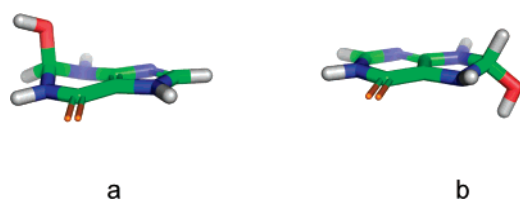


Figure 2. (a) Structure of 6-mercaptapurine tetrahedral intermediate **2oh_n7h**. (b) Structure of 6-mercaptapurine tetrahedral intermediate **8oh_n1h**.

Finally, we tested our ability to predict the major metabolites using energies of the tetrahedral intermediates for a number of chemicals reported in the literature by Krenitsky et al.²⁰ to be both AO and XO substrates. While it is generally believed that the mechanism of AO and XO oxygenations are similar, this is not an entirely valid assumption because differing substrate specificities exist for each. These differences are likely dictated by factors including the protonation state of the MoCo and amino acid variations at the enzyme active site of each.^{17,20} Krenitsky et al. examined the specificity of AO and XO with regard to the hydroxylation of a number of substrates. The authors concluded that both enzymes have some features in common because they oxidized some of the same compounds, although they did note that different oxidation products resulted

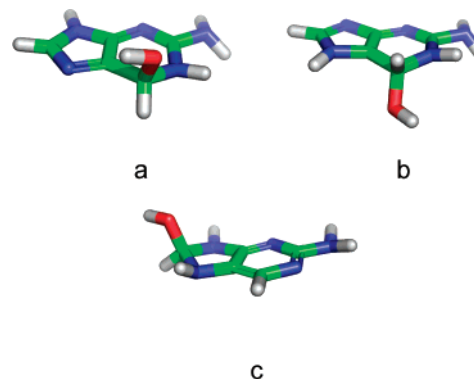


Figure 3. (a) Structure of 2-aminopurine tetrahedral intermediate **6oh_n9h** with $-OH$ on C6 forming a possible favorable interaction with the lone pair on N7. (b) Structure of 2-aminopurine tetrahedral intermediate **6oh_n7h**. (c) Structure of 2-aminopurine tetrahedral intermediate **8oh**.

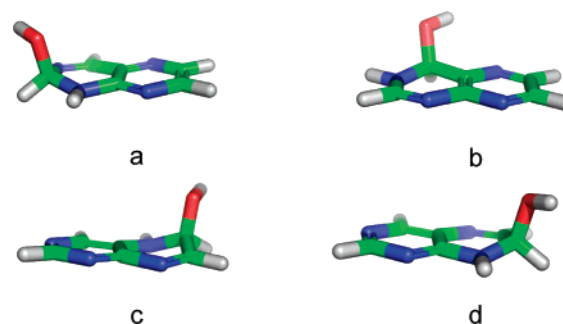


Figure 4. Structures of pteridine tetrahedral intermediates **2oh** (a), **4oh** (b), **6oh** (c), and **7oh** (d).

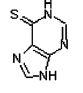
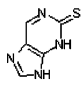
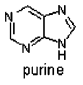
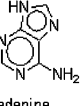
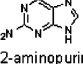
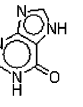
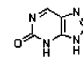
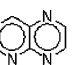
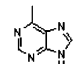
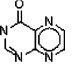
in many instances. We attempted to reproduce the sites of oxidation of the substituted azaheterocycles examined by Krenitsky et al. (Table 3 of ref 20). The relative energies of the likely tetrahedral intermediates for each compound examined

Table 2. Relative Energy Comparisons^a between Likely Tetrahedral Intermediates of Proprietary Druglike Molecules

Substrate	Site of Oxidation	Substrate	Site of Oxidation		
Compound 1	2oh^b	$\Delta G_{rel} = 0$ kcal/mol	Compound 1a ^c	2oh	$\Delta G_{rel} = 0$ kcal/mol
	2'oh_n1h	$\Delta G_{rel} = +3.50$ kcal/mol		2'oh_n1h	$\Delta G_{rel} = +2.42$ kcal/mol
	2'oh_n3h	$\Delta G_{rel} = +7.41$ kcal/mol		2'oh_n3h	$\Delta G_{rel} = +6.96$ kcal/mol
Compound 2	2oh^b	$\Delta G_{rel} = 0$ kcal/mol	Compound 2a ^c	2oh	$\Delta G_{rel} = 0$ kcal/mol
	6oh	$\Delta G_{rel} = +12.54$ kcal/mol		6oh	$\Delta G_{rel} = +11.78$ kcal/mol
Compound 3	2oh^b	$\Delta G_{rel} = 0$ kcal/mol	Compound 3a	2oh^b	$\Delta G_{rel} = 0$ kcal/mol
	7oh	$\Delta G_{rel} = +3.23$ kcal/mol		7oh	$\Delta G_{rel} = +2.15$ kcal/mol
Compound 3b	2oh^b	$\Delta G_{rel} = 0$ kcal/mol	Compound 3c	2oh^b	$\Delta G_{rel} = +0$ kcal/mol
	7oh	$\Delta G_{rel} = +1.57$ kcal/mol		7oh	$\Delta G_{rel} = +1.47$ kcal/mol
Compound 3d ^b	2oh^b	$\Delta G_{rel} = 0$ kcal/mol			
	7oh	$\Delta G_{rel} = +2.76$ kcal/mol			

^a In kcal/mol. ^b Observed site of metabolism. ^c Truncated model of compound in series where the metabolite is predicted.

Table 3. Relative Energy Comparisons^a between Likely Tetrahedral Intermediates of Xanthine Oxidase and Aldehyde Oxidase Metabolism^b

Substrate	Site of Oxidation	Substrate	Site of Oxidation		
 6-mercaptapurine	8 → 2 (XO)	8 (AO)	 2-mercaptapurine	8 (XO)	6 (AO)
	2oh_n7h	$\Delta G_{rel} = 0$ kcal/mol		6oh_n9h	$\Delta G_{rel} = +3.77$ kcal/mol
	2oh_n3h	$\Delta G_{rel} = +10.04$ kcal/mol		6oh_n7h	$\Delta G_{rel} = 0$ kcal/mol
	8oh_n1h	$\Delta G_{rel} = +0.12$ kcal/mol		8oh_n1h	$\Delta G_{rel} = +7.53$ kcal/mol
	8oh_n3h	$\Delta G_{rel} = +18.28$ kcal/mol		8oh_n3h	$\Delta G_{rel} = +17.33$ kcal/mol
 purine	6 → 2 → 8 (XO)	8 (AO)	 adenine	8 → 2 (XO)	8 (AO)
	2oh_n1h	$\Delta G_{rel} = +12.24$ kcal/mol		2oh_n1h	$\Delta G_{rel} = +12.73$ kcal/mol
	2oh_n3h	$\Delta G_{rel} = +11.84$ kcal/mol		2oh_n3h	$\Delta G_{rel} = +6.49$ kcal/mol
	6oh	$\Delta G_{rel} = +1.45$ kcal/mol		8oh	$\Delta G_{rel} = 0$ kcal/mol
 2-aminopurine	6 (XO)	8 (AO)	 hypoxanthine	8 → 2 (XO)	2 (AO)
	6oh_n7h	$\Delta G_{rel} = +8.86$ kcal/mol		2oh	$\Delta G_{rel} = 0$ kcal/mol
	6oh_n9h	$\Delta G_{rel} = +3.02$ kcal/mol		8oh	$\Delta G_{rel} = +3.19$ kcal/mol
 2-hydroxypurine	8 → 6 (XO)	6 (AO)	 pteridine	4,2,7 (XO)	4,2 (AO)
	6oh	$\Delta G_{rel} = 0$ kcal/mol		2oh	$\Delta G_{rel} = +1.17$ kcal/mol
	8oh	$\Delta G_{rel} = +4.43$ kcal/mol		4oh	$\Delta G_{rel} = 0$ kcal/mol
 6-methylpurine	Not metab. (XO)	8 (AO)	 4-hydroxypteridine	2,7 (XO)	2 (AO)
	2oh_n1h	$\Delta G_{rel} = +8.79$ kcal/mol		2oh	$\Delta G_{rel} = 0$ kcal/mol
	2oh_n3h	$\Delta G_{rel} = +11.40$ kcal/mol		6oh	$\Delta G_{rel} = +7.10$ kcal/mol
	8oh	$\Delta G_{rel} = 0$ kcal/mol	7oh	$\Delta G_{rel} = +5.05$ kcal/mol	

^a In kcal/mol. ^b Arrow indicates the order of oxidation (see Table 3 of ref 20 for further details).

are shown in Table 3. Overall, the energy of the tetrahedral intermediates predicted the site of oxygenation for AO but not for XO. In most instances, the differences in energy between the likely tetrahedral intermediates in Table 3 are substantial, and interpretation is straightforward. However, in some cases the energy differences are relatively small.

The experimentally observed product of 6-mercaptapurine AO metabolism is oxygenation of position 8 in the ring. The results of the DFT calculations suggest that metabolism would be favored at position 2 in the ring (**2oh_n7h**), where this intermediate is only 0.12 kcal/mol lower in energy than the tetrahedral intermediate of the observed product tetrahedral intermediate **8oh_n1h**. Interestingly both metabolites are seen with XO (Figure 2), so the small difference in energy is likely to be relatively accurate.

When the likely intermediates of AO metabolism for 2-aminopurine at position 6 were considered, a considerable difference in the energy was found. This difference appeared to be due

primarily to the location of the hydrogen on the imidazole portion of the fused heterocycle in the intermediate structure as both tautomeric (hydrogen on N7 or N9) structures were examined. If the hydrogen atom was located on N7 (**6oh_n7h**), the energy of the optimized tetrahedral intermediate was 5.84 kcal/mol higher than if the hydrogen atom was located on N9 (**6oh_n9h**). From an examination of the two structures, the energy difference can be attributed in part to the hydrogen of the -OH group of the **6oh_n9h** intermediate forming an apparently favorable electrostatic interaction with the N7 (and related puckering in the pyrimidine ring portion of this 2-aminopurine intermediate) with an O-H...N angle of 104.4°. This interaction is not possible in the **6oh_n7h** intermediate as the hydrogen of the OH is directed away from the NH, where the O-H...N angle is 25.8° (Figure 3).

Here, the energy difference in tetrahedral intermediate structures, although substantial, would not affect the prediction results because the lowest energy tetrahedral intermediate in

this series corresponds to the **8oh** structure, which is the observed oxygenation product of AO metabolism.

In the case of pteridine, the experimentally observed products of AO result from oxygenation of positions 4 and 2 in the ring, while the observed products of XO are derived from oxygenation at positions 4, 2, and 7. The results of the DFT calculations suggest that metabolism would be favored at position 4 over that at position 7 by 0.57 kcal/mol and position 2 by 1.17 kcal/mol. Here again, the small differences in energy appear to be relatively accurate in predicting the product. A favorable electrostatic interaction between the $-OH$ on position 4 and the N5 with an NH distance of 2.7 Å and an $O-H\cdots N$ angle of 99.1° does not appear likely in the case of the **4oh** intermediate (Figure 4). The correct major metabolite was predicted; however, the method was unable to predict both major metabolites of pteridine by AO if rank ordering of intermediates was considered. Interestingly, the metabolite of 4-hydroxypteridine was correctly predicted using this method.

Discussion

Determination and optimization of metabolism represent a major bottleneck in drug discovery. In particular, the cytochrome P450 enzyme system is often responsible for a large first-pass effect or bioactivation to potentially toxic reactive intermediates. To circumvent these metabolic problems, in particular aromatic hydroxylation, it is becoming common practice to replace a carbon atom in the aromatic ring with a nitrogen atom. These azaheterocycles are relatively inert to cytochrome P450 mediated oxidations because of the electron-withdrawing effects of the nitrogen. These electron-deficient carbon atoms can become targets for nucleophilic oxygenation by xanthine and aldehyde oxidases. Thus, new generation drugs are more likely to be XO and AO substrates. At present it is not known if XO and AO can bioactivate molecules, but these enzymes in general have higher turnover numbers than the P450 enzymes and may play a role in first-pass effects.

The computational method presented in this manuscript is the first method for predicting regioselectivity in AO-catalyzed reactions. The method is very accurate considering it assumes no interaction with the protein. Overall, from reports in the literature on druglike or drug molecules (Table 1), new generation lead compounds (Table 2), and small molecules (Table 3), the predictive capability is 93%, or 25 out of 27 major metabolites predicted for AO. In the two cases that the major metabolites are not predicted correctly, only 0.12 and 0.73 kcal/mol separate the predicted and actual metabolite. This is in contrast to the large difference in energy (in general >3 kcal/mol) for the majority of the compounds tested. The method fails to predict XO regioselectivity, only correctly predicting 44% of the major metabolites for XO.

One potential problem with this method is that a number of these compounds can exist in more than one tautomer, and computational predictions of regioselectivity are dependent on which tautomer is used. From our calculations thus far, it appears that using the lowest energy tautomer in the gas-phase results in the correct answer. Another potential problem is when intramolecular hydrogen bonds can form. These intramolecular interactions lower the energy of the tetrahedral intermediate and in one case, deoxypenciclovir (Figure 1), result in an incorrect prediction of the major metabolite. A more complete enzyme model would most likely correct this problem.

It is interesting that the energy of the tetrahedral intermediate is predictive for AO but not for XO. This is not surprising

as XO has specific endogenous substrates and perhaps a more specific binding interaction with the substrate. What is surprising is that the methods work so well for AO. The ability to predict the major metabolite based solely on the electronic features indicates that the substrates are able to sample a number of different binding modes and that the reaction most likely proceeds through the lowest energy electronic pathway, with the enzyme playing very little role in orientation. This means either the enzyme is very flexible and can bind molecules in multiple binding modes or the enzyme does not truly bind the substrate but instead just presents the electrophilic carbon to oxygen bond to the Mo cofactor. The latter binding mode would make it difficult for the enzyme to catalyze the reaction by hydrogen-bonding interactions. These results are very similar to those seen for P450 3A4 because for 3A4 regioselectivity appears to be dominated by electronic features. However, regioselectivity predictions for 3A4 rarely exceed 80% with any given model.^{14–16}

The failure of the method to predict XO regioselectivity is most likely a result of specific hydrogen bonds to the nitrogen adjacent to the electrophilic carbon. A hydrogen bond to a particular nitrogen in the molecule would stabilize the binding mode and increase the electrophilicity of the carbon. Given the differences in reactivity between XO and AO, generalizing the mechanism of the molybdenum containing oxygenases may not be warranted without further investigation.

The results presented here provide a very optimistic picture with regard to drug design and metabolite prediction. The method, while still only tested on a limited set of substrates, is highly predictive, and blocking the predicted site of metabolism should alter the metabolic profile. Furthermore, the method can be used to guide the synthesis of the major metabolite, obviating the need to make all the possible metabolites.

Conclusions

This study describes a simple qualitative method to predict the likely metabolite resulting from biotransformation by aldehyde oxidase. The calculations suggest that oxidation of substrates by AO appears to be due primarily to the electronic effects of the substituents, as previously suggested.²⁰ This approach provides a rank ordering of likely products by examining the tetrahedral intermediate in the metabolism of these compounds via AO with $>90\%$ accuracy for the compounds examined. The method also appears to be largely successful in distinguishing the products of XO metabolism from those of AO metabolism for a number of closely related purine derivatives.

This model should be useful when the observed metabolic profile for a molecule is inappropriate because of either an undesirable metabolite or an inappropriate rate of metabolism. A predictive model for regioselectivity can be used to both identify the likely site of metabolism and suggest modifications to alter that metabolism. Although the available data cannot be used to model rates of AO metabolism, the observed regioselectivity is an indication of the relative rates of metabolism within a molecule. Therefore, electronic features that can alter regioselectivity may be important for predicting rates as well. Additional kinetic data will be needed to test this hypothesis.

It is important to note that the rank ordering and conclusions did not change following inclusion of the frequency calculation or higher basis set corrections; therefore, the method appears to be equally effective without these computationally expensive corrections.

Computational Methodology

Tetrahedral intermediate structures were generated by considering the geometry-optimized, neutral substrate, unless otherwise noted, where the nucleophile, OH^- attacks a carbon atom. For nitrogen-containing heterocycles, a hydrogen atom was added to the nitrogen, resulting in a net addition of water, in accordance with the proposed mechanism. All geometries and energies reported in this study were computed using the B3LYP density functional theory method^{21–24} implemented in the Gaussian03 program package.²⁵ Geometry optimizations were performed using the 6-31G(d,p) basis set and were spin-unrestricted. Single-point calculations on the optimized geometries were performed with the larger basis set 6-311+G(2d,-2p) to obtain more accurate energy values. Typical errors observed for the B3LYP functional are in the range of 2–3 kcal/mol in calculations of reaction barriers and for complexes that do not contain transition metals,^{26–30} which may vary depending on the reaction being examined. Hessians were determined at the B3LYP/6-31G(d,p) level. Complete thermochemical calculations were performed, and final energies reported include zero-point vibrational energies. The frequency calculations also served to verify that a stationary point was achieved, i.e., no negative eigenvalues for minima. Atomic charges were calculated using the ESP method of Merz and Kollman³¹ implemented in Gaussian03. Figures were made in PyMOL.³²

Acknowledgment. The authors thank Robert Sheridan for helpful discussions. R.A.T. and J.P.J. thank the National Institutes of Health (Grant ES09122) for funding.

References

- Beedham, C. The Role of Non-P450 Enzymes in Drug Oxidation. *Pharm. World Sci.* **1997**, *19*, 255–263.
- Obach, R. S.; Huynh, P.; Allen, M. C.; Beedham, C. Human Liver Aldehyde Oxidase: Inhibition by 239 Drugs. *J. Clin. Pharmacol.* **2004**, *44*, 7–19.
- Obach, R. S.; Walsky, R. L. Drugs That Inhibit Oxidation Reactions Catalyzed by Aldehyde Oxidase Do Not Inhibit the Reductive Metabolism of Ziprasidone to Its Major Metabolite, S-Methylidihydroziprasidone: An in Vitro Study. *J. Clin. Psychopharmacol.* **2005**, *25*, 605–608.
- Obach, R. S. Potent Inhibition of Human Liver Aldehyde Oxidase by Raloxifene. *Drug Metab. Dispos.* **2004**, *32*, 89–97.
- Terao, M.; Kurosaki, M.; Barzago, M. M.; Varasano, E.; Boldetti, A.; Bastone, A.; Fratelli, M.; Garattini, A. Avian and Canine Aldehyde Oxidases: Novel Insights into the Biology and Evolution of Molybdo-flavoenzymes. *J. Biol. Chem.* **2006**, *281*, 19748–19761.
- Huang, D.-Y.; Furukawa, A.; Ichikawa, Y. Molecular Cloning of Retinal Oxidase/Aldehyde Oxidase cDNAs from Rabbit and Mouse Livers and Functional Expression of Recombinant Mouse Retinal Oxidase cDNA in *Escherichia coli*. *Arch. Biochem. Biophys.* **1999**, *364*, 264–272.
- Berger, R.; Mezey, E.; Clancy, K. P.; Harta, G.; Wright, R. M.; Repine, J. E.; Brown, R. H.; Brownstein, M.; Patterson, D. Analysis of Aldehyde Oxidase and Xanthine Dehydrogenase/Oxidase as Possible Candidate Genes for Autosomal Recessive Familial Amyotrophic Lateral Sclerosis. *Somatic Cell Mol. Genet.* **1995**, *21*, 121–131.
- Panoutsopoulos, G. I.; Beedham, C. Kinetics and Specificity of Guinea Pig Liver Aldehyde Oxidase and Bovine Milk Xanthine Oxidase Towards Substituted Benzaldehydes. *Acta Biochim. Pol.* **2004**, *51*, 649–663.
- Kawashima, K.; Hosoi, K.; Naruke, T.; Shiba, T.; Kitamura, M.; Watabe, T. Aldehyde Oxidase-Dependent Marked Species Difference in Hepatic Metabolism of the Sedative-Hypnotic, Zaleplon, between Monkeys and Rats. *Drug Metab. Dispos.* **1999**, *27*, 422–428.
- Rashidi, M. R.; Smith, J. A.; Clarke, S. E.; Beedham, C. In Vitro Oxidation of Famciclovir and 6-Deoxyfamciclovir by Aldehyde Oxidase from Human, Guinea Pig, Rabbit, and Rat Liver. *Drug Metab. Dispos.* **1997**, *25*, 805–813.
- Hille, R. Molybdenum-Containing Hydroxylases. *Arch. Biochem. Biophys.* **2005**, *433*, 107–116.
- Enemark, J. H.; Cooney, J. J. A.; Wang, J.-J.; Holm, R. H. Synthetic Analogues and Reaction Systems Relevant to the Molybdenum and Tungsten Oxotransferases. *Chem. Rev.* **2003**, *104*, 1175–1200.
- Massey, V.; Harris, C. M. Milk Xanthine Oxidoreductase: The First One Hundred Years. *Biochem. Soc. Trans.* **1997**, *25*, 750–755.
- Sheridan, R. P.; Korzekwa, K. R.; Torres, R. A.; Walker, M. J. Empirical Regioselectivity Models for Human Cytochromes P450 3A4, 2D6, and 2C9. *J. Med. Chem.* **2007**, *50*, 3173–3184.
- Singh, S. B.; Shen, L. Q.; Walker, M. J.; Sheridan, R. P. A Model for Predicting Likely Sites of CYP3A4-Mediated Metabolism on Drug-like Molecules. *J. Med. Chem.* **2003**, *46*, 1330–1336.
- Cruciani, G.; Carosati, E.; De Boeck, B.; Ethirajulu, K.; Mackie, C.; Howe, T.; Vianello, R. MetaSite: Understanding Metabolism in Human Cytochromes from the Perspective of the Chemist. *J. Med. Chem.* **2005**, *48*, 6970–6979.
- Beedham, C. Molybdenum Hydroxylases: Biological Distribution and Substrate–Inhibitor Specificity. *Progress in Medicinal Chemistry*; Elsevier Science Publishers, B.V.: London, 1987.
- Okamoto, K.; Matsumoto, K.; Hille, R.; Eger, B. T.; Pai, E. F.; Nishino, T. The Crystal Structure of Xanthine Oxidoreductase during Catalysis: Implications for Reaction Mechanism and Enzyme Inhibition. *Proc. Natl. Acad. Sci. U.S.A.* **2004**, *101*, 7931–7936.
- Hammond, G. S. A Correlation of Reaction Rates. *J. Am. Chem. Soc.* **1955**, *77*, 334–338.
- Krenitsky, T. A.; Neil, S. M.; Elion, G. B.; Hitchings, G. H. A Comparison of the Specificities of Xanthine Oxidase and Aldehyde Oxidase. *Arch. Biochem. Biophys.* **1972**, *150*, 585–599.
- Becke, A. D. Density-Functional Exchange-Energy Approximation with Correct Asymptotic Behavior. *Phys. Rev.* **1988**, *A38*, 3908–3100.
- Becke, A. D. Density-Functional Thermochemistry. III. The Role of Exact Exchange. *J. Chem. Phys.* **1993**, *98*, 5648–5652.
- Becke, A. D. Density-Functional Thermochemistry. I. The Effect of the Exchange-Only Gradient Correction. *J. Chem. Phys.* **1992**, *96*, 2155–2160.
- Becke, A. D. Density-Functional Thermochemistry. II. The Effect of the Perdew–Wang Generalized-Gradient Correlation Correction. *J. Chem. Phys.* **1992**, *97*, 9173–9177.
- Frisch, M. J.; Trucks, G. W.; Schlegel, H. B.; Scuseria, G. E.; Robb, M. A.; Cheeseman, J. R.; Zakrzewski, V. G.; Montgomery, J. A., Jr.; Stratmann, R. E.; Burant, J. C.; Dapprich, S.; Millam, J. M.; Daniels, A. D.; Kudin, K. N.; Strain, M. C.; Farkas, O.; Tomasi, J.; Barone, V.; Cossi, M.; Cammi, R.; Mennucci, B.; Pomelli, C.; Adamo, C.; Clifford, S.; Ochterski, J.; Petersson, G. A.; Ayala, P. Y.; Cui, Q.; Morokuma, K.; Malick, D. K.; Rabuck, A. D.; Raghavachari, K.; Foresman, J. B.; Cioslowski, J.; Ortiz, J. V.; Stefanov, B. B.; Liu, G.; Liashenko, A.; Piskorz, P.; Komaromi, I.; Gomperts, R.; Martin, R. L.; Fox, D. J.; Keith, T.; Al-Laham, M. A.; Peng, C. Y.; Nanayakkara, A.; Gonzalez, C.; Challacombe, M.; Gill, P. M. W.; Johnson, B. G.; Chen, W.; Wong, M. W.; Andres, J. L.; Head-Gordon, M.; Replogle, E. S.; Pople, J. A. *Gaussian 03*, revision C.01; Gaussian, Inc.: Wallingford, CT, 2004.
- Bauschlicher, C. W. J. A Comparison of the Accuracy of Different Functionals. *Chem. Phys. Lett.* **1995**, *246*, 40–44.
- Guner, V.; Khuong, K. S.; Leach, A. G.; Lee, P. S.; Bartberger, M. D.; Houk, K. N. A Standard Set of Pericyclic Reactions of Hydrocarbons for the Benchmarking of Computational Methods: The Performance of ab Initio, Density Functional, CASSCF, CASPT2, and CBS-QB3 Methods for the Prediction of Activation Barriers, Reaction Energetics and Transition State Geometries. *J. Phys. Chem. A* **2003**, *107*, 11445–11459.
- Grimme, S. Improved Second-Order Møller–Plesset Perturbation Theory by Separate Scaling of Parallel- and Antiparallel-Spin Pair Correlation Energies. *J. Chem. Phys.* **2003**, *118*, 9095–9102.
- Lynch, B. J.; Truhlar, D. G. How Well Can Hybrid Density Functional Methods Predict Transition State Geometries and Barrier Heights? *J. Phys. Chem. A* **2001**, *105*, 2936–2941.
- Koch, W.; Holthausen, M. C. *A Chemist's Guide to Density Functional Theory*, 2nd ed.; Wiley-VCH: Weinheim, Germany, 2001.
- Besler, B. H.; Merz, K. M. J.; Kollman, P. A. Atomic Charges Derived from Semiempirical Methods. *J. Comput. Chem.* **1990**, *11*, 431–439.
- DeLano, W. L. *The PyMOL Molecular Graphics System*, version 0.98; DeLano Scientific: San Carlos, CA.

JM0703690